Beni-Suef University Journal of Basic and Applied Sciences

RESEARCH

Open Access

Profiling of insulin and resveratrol interaction using multi-spectroscopy and molecular docking study

Sahri Yanti[1,2], Wei-Jyun Chien[1*] and Dinesh Chandra Agrawal[1,3]

Abstract

Background: Resveratrol, a phenolic compound, has various medicinal properties, including anticancer, anti-diabetic, antioxidant, anti-inflammatory, etc. Diabetes is a killing disease, especially for people who cannot maintain a healthy lifestyle. People with diabetes need additional information about a supplement that can prevent and treat diabetes. The present study aims to investigate the interaction of insulin with resveratrol using fluorescence spectroscopy, UV–Vis spectroscopy, CD spectropolarimeter, and molecular docking methods. As an outcome of this study, we expect to understand the contribution of resveratrol in insulin resistance.

Result: The fluorescence spectroscopy results showed that the peak intensity of insulin emission decreased with resveratrol. The interaction of insulin with resveratrol involved a combination of static and dynamic quenching effects. Temperature changes caused the binding constant (*K*) and the binding site (*n*) unstable. The interaction occurred through hydrogen bonding, van der Waal, and was hydrophobic. The results of UV–Vis spectroscopy showed that the addition of resveratrol caused a peak in a blueshift, and the absorbance was hyperchromic. Also, there was a reduction in electron transition and the extinction coefficient. The CD spectropolarimeter results showed that the addition of resveratrol affected the secondary structure of insulin. The amount of α-helix and β-sheet slightly change and increase in the secondary structure's length. The molecular docking study showed that resveratrol interacts via hydrogen bonding with glycine and asparagine. van der Waal interactions occurred in asparagine, phenylalanine, and cysteine. The interaction of electrons occurred through the π orbitals of resveratrol with tyrosine A and B. The binding energy of molecules interaction happened spontaneously on a hydrophobic surface.

Conclusion: Profiling the interaction of insulin and resveratrol shows that resveratrol can stabilize insulin structure and prevent insulin resistance in diabetes.

Keywords: Insulin, Resveratrol, Binding energy, Binding site, Molecular docking

1 Background

Resveratrol has various medicinal properties such as neuroprotective, chemopreventive, cardioprotective, anticancer, anti-diabetic, antioxidant, and anti-inflammatory [1, 2]. Resveratrol, as an anti-inflammatory agent, inhibits the decay of teeth supporting tissues [3]. The benefits of resveratrol have been correlated with the molecular structure that can bind to other molecules. Resveratrol has two aromatic rings linked by a styrene double bond [2]. The number of hydroxyl groups distinguishes the aromatic ring. The *cis*-resveratrol and *trans*-resveratrol depend on the molecule's position attached to the styrene double bond. *Trans*-resveratrol has two derivatives, RSV1 and RSV2 (as shown in Fig. 1). The *cis* and *trans* isomers of the resveratrol are unstable, and their changes are influenced by light [4]. The inhibition process in cells

*Correspondence: wjchien@gm.cyut.edu.tw

[1] Department of Applied Chemistry, Chaoyang University of Technology, 168, Jifeng E. Rd., Wufeng District, Taichung City 413310, Taiwan
Full list of author information is available at the end of the article

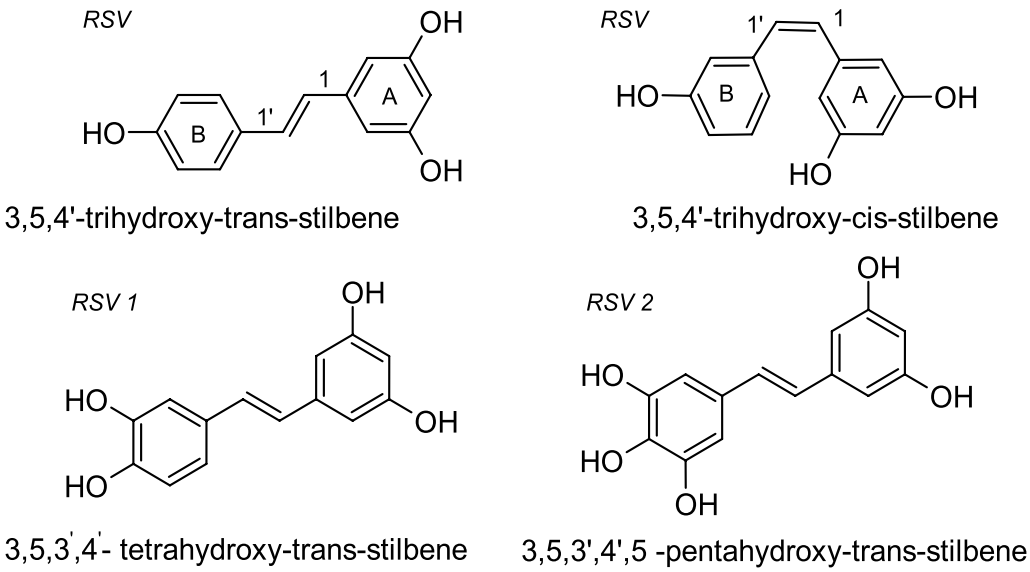

Fig. 1 Chemical structure of resveratrol

is due to three hydroxyl groups on RSV2 [5]. Even in minor quantities, resveratrol could inhibit certain infections [2]. Resveratrol is a secondary metabolite found in certain plants, such as *Veratrum grandiflorum* [6], grapes for red wine production [2, 7], peanut oil, soybean oil, corn oil, and colza oil [8–10], cashew nut [11]. Identification of resveratrol has been carried out in our unpublished research. Resveratrol is found in candlenut oil, peanut oil, sesame oil, sunflower oil, sacha inchi press residue oil, and black beans oil. Among these, sesame oil has the highest levels of resveratrol [].

Resveratrol, an anti-obesity supplement, facilitates glucose transport in human fat cells and reduces adipose tissue mass [12, 13]. Glucose transport is also associated with diabetes caused by increased blood sugar levels, impaired insulin secretion, and resistance action of insulin. To cure type 2 diabetes (T2D), resveratrol doses exceeding 100 mg/d were found to be optimal for diabetic patients [14]. Resveratrol has been reported to reduce insulin resistance and glycosylated hemoglobin significantly [1]. Hereditary diseases triggered by insulin resistance are obesity-T2D, non-alcoholic fatty liver disease, polycystic ovary syndrome, and atherosclerotic cardiovascular disease [15]. Obesity and diabetes scourge women aged 20–39 years [16]. The total number of people with diabetes in the USA is 37.3 million (11.3% of the total US population) [17]. Given the high number of diabetic patients and the ability of resveratrol to act as an anti-diabetic agent, profiling the interaction of these two molecules would be an important study. Several researchers have reported the interaction of resveratrol with protein molecules. These proteins are in the form of DNA sequences [18], trypsin [19], bovine serum albumin [20], human serum albumin [21], insulin [4, 22].

Resveratrol interacts spontaneously with DNA sequences, bovine serum albumin (BSA), human serum albumin (HSA), trypsin, and insulin. These proteins are connected through hydrogen bonds, electrostatic, and hydrophobic. Resveratrol binds with DNA and changes the DNA conformation moderately. Resveratrol has the potential for DNA sensing probes [18]. The interaction of BSA and HSA with resveratrol illustrates the distribution of the drug-protein complex in the blood. Serum albumin plays a vital role in transporting nutrients and drugs. BSA is serum albumin from cattle, and its physicochemical properties are similar to HAS [23]. Meanwhile, resveratrol interaction with trypsin is recommended for the food industry because it can inhibit protease activity [19].

Resveratrol has been reported to affect insulin dysregulation in the blood of Goto-Kakizaki (GK) rats with congenital type 2 diabetes. Insulin binding occurs in skeletal muscle and liver. A significant effect was also observed in reducing protein expression related to the blood glucose amount [22]. The interaction of resveratrol with bovine insulin is spontaneous and exothermic. The appearance of hydrogen bonds was observed through fluorescence spectroscopy by the peak shift from 283 to 286 nm. The reduction of insulin emission indicates that insulin emission has been quenched. Fluorescence is more sensitive than absorption. The tyrosine residue of insulin has an important role in polarity. The presence of resveratrol has reduced the α-helix structure of the insulin structure,

breaking the dimeric insulin structure into monomers [4]. Bovine insulin has also interacted with paclitaxel [24], DPPC (dipalmitoylphosphatidylcholine), or POCP (1-palmitoyl-2-oleoylphosphatidylcholine) [25]. At the same time, human insulin has interacted with vanillin [26], vitamin E, and vitamin D3 [27].

The researchers used human and bovine insulin from the various insulin interaction analyses. Insulin in the pancreas has a hexameric structure, each hexamer has three dimers, and the dimer is formed by combining two monomers. Compared with hexamers and dimers, insulin is active in the form of monomers. The terminal C fragment of insulin B has the same function as insulin in the monomer form [28]. In this study, profiling was carried out using insulin chain B to interact with resveratrol at a pH suitable for insulin in the pancreas (pH 7.4), and completed with 3D interaction using molecular docking.

The regulation of fat and carbohydrate metabolism is controlled by peptide hormones such as insulin [29]. The insulin molecule consists of 51 amino acids divided into chains A and B. These chains are linked together by sulfide bridges. Chain B has a helix structure [30]. The insulin complex is formed through monomers binding, forming dimers and hexamers [31]. Insulin in the monomer form has a heterogeneous and irregular conformation. This affects the biological activity and lifetime of pharmaceutical formulations [32]. The process of insulin fibrillation can occur in diabetic patients. Small molecules, peptides, and surfactants can inhibit insulin fibrillation [24]. Studies on the interaction of insulin with various small molecules have been carried out, such as vanillin [26], phloretin [33], resveratrol [4], vitamin E, and vitamin D3 [27], paclitaxel [24], DPPC (dipalmitoylphosphatidylcholine) or POCP (1-palmitoyl-2-oleoylphosphatidylcholine) [25].

Thermodynamic and kinetic observations of the interaction of insulin with ligands have been carried out using various combinations of spectroscopy such as fluorescence spectroscopy and UV–Vis spectroscopy. Verdian et al. applied fluorescence and UV–Vis spectroscopy to observe the behavior of insulin with its aptamer [29]. The interaction between insulin and phloretin and resveratrol has been carried out using a combination of UV–Vis spectroscopy, fluorescence spectroscopy, and CD spectropolarimeter [4, 33]. A combination of CD spectropolarimeter and atomic force microscopy (AFM) was applied to determine the paclitaxel effect on insulin fibrillation [24]. Insulin and resveratrol have been reported to interact through hydrogen bonds and van der Waals [4] spontaneously. The bonds formed between protein and ligands are seen in three dimensions (3D) using molecular docking studies. The interaction of insulin with phloretin in 3D shows connections by hydrogen bonds. The binding site was at the Tyr14 (tyrosine) and Glu17 (glutamic acid) [33]. Given this background, the present study aims to investigate the interaction of insulin with resveratrol using fluorescence spectroscopy, UV–Vis spectroscopy, CD spectropolarimeter, and molecular docking methods. Also, we aim to profile the effect of resveratrol on insulin interaction and determine the position of the binding site, binding residue, and binding energy. As an outcome of this study, we expect to understand the contribution of resveratrol to insulin resistance.

2 Methods

Insulin Chain B Oxidized From Bovine Pancreas CAS 30003726, 3495.89 g/mol (Sigma Aldrich), Resveratrol CAS 501360, 228.24 g/mol (Sigma Aldrich), phosphate buffer (pH 7.4), methanol 99.5% (Merck) were used in the study. The instruments utilized were analytical balance (AND GR-200), UV–Vis spectrometer (PerkinElmer Lambda 265), fluorescence spectrometer (Jasco FP-750 with Xenon), stabilizer temperature water tank (FIRSTEK Model-B403H), fluorescent holder (Jasco STR-312), CD spectropolarimeter (Jasco J-815 with a 150 W Xenon), and a 1-ml quartz cuvette. Data were processed using Origin and Microsoft Excel software.

2.1 Fluorescence spectroscopy procedure

Resveratrol and insulin were diluted using phosphate buffer pH 7.4 and methanol. Standard stock solution for resveratrol was prepared in 11.412 mg/100 ml methanol and insulin in 1.748 mg/10 ml buffer. The insulin concentration was fixed at 5.0×10^{-5} M, and initial resveratrol concentration was increased from 5.0×10^{-7} to 5.0×10^{-4} M. The INS-RSV solutions were prepared with different molar ratios of resveratrol (1:10; 1:5; 1:2.5; 1:1.25; 1:1; 1:0.5; 1:0.25; 1:0.125; 1:0.1; 1:0.05; 1:0.025; 1:0.0125; 1:0.01).

2.2 UV–Vis spectroscopy procedure

The INS-RSV solutions have various molar ratios of resveratrol with an initial concentration increased from 5.0×10^{-7} to 5.0×10^{-4} M. Record UV–Vis spectrometer using 1-ml quartz cuvette.

2.3 Circular dichroism spectropolarimeter procedure

The insulin concentration was constant at 5.0×10^{-5} M, and initial resveratrol concentration was increased from 5.0×10^{-7} to 5.0×10^{-4} M. The INS-RSV solutions were taken into a 1-ml quartz cuvette and inserted into CD Spectropolarimeter. Secondary structure analysis was conducted online through the DichroWeb website. The software used was SELCON 3 by Sreerama and Woody.

2.4 Molecular docking analysis

The molecular docking was performed using AutoDock MGL Tools, AutoDock Vina, and Discovery studio software. Simulations were done on human insulin code pdb1a7f obtained from the protein databank and resveratrol code CID 445,154 from PubChem. Overall, the flowchart of methods is shown in Fig. 2.

3 Results

Fluorescence spectroscopy has a high sensitivity. It can analyze samples at a minimum concentration of 10^{-9} M, and up to 10^{-12} M [34]. In this study, the analyte concentration range used was $10^{-7} - 10^{-4}$ M. Figure 3 shows the different spectra between insulin, resveratrol, and INS-RSV solution.

The relationship of fluorescence intensity of INS-RSV with resveratrol is shown in Fig. 4a, while Fig. 4b, c is used to determine thermodynamic and kinetic parameters and the result is shown in Table 1.

UV–Vis spectroscopy analysis aims to determine the maximum absorbance wavelength in INS-RSV solution. It also aims to determine the value of the extinction coefficient involved in the interaction. Analysis using UV–Vis spectroscopy was carried out by keeping the polypeptide in a constant concentration [29]. The results of UV–Vis spectroscopy are presented in Fig. 5 and Table 2.

Observation of the interaction of insulin and resveratrol using a CD spectropolarimeter aims to determine the effect of resveratrol on the secondary structure of insulin. The secondary structures of insulin are α-helix, β-turn and other, and random coil [33, 35]. Insulin monomer has an α-helix structure in chains A and B and is connected by disulfide bridges [32]. The 3D image of insulin is shown in Fig. 7. The change in secondary structure is shown in Fig. 6 and Table 3. The visualization of binding residue and binding site in insulin and resveratrol interaction is shown in Fig. 7. Also, the binding energy is shown in Table 4.

4 Discussion

4.1 Fluorescence spectroscopy

The analysis of the interaction of insulin and resveratrol is closely related to the sensitivity of the molecule to radiation exposure and supramolecular concepts. Radiation exposure causes absorption, and electrons transition from the ground to the excited state. The average lifetime of the electron transition in the excited state is 10^{-5}–$10.^{-8}$ s. An excited state is unstable. After that, the electrons will return to the ground state through the luminescence process. Luminescence occurs by releasing energy (relaxation) while emitting light, detected at wavelengths greater than absorption and excitation. Luminescence is also known as fluorescence. The fluorescence spectra are always broad because there are many vibrational states. Not all chemical compounds have luminescence properties; treating them to make them luminescent is necessary. Compounds that have

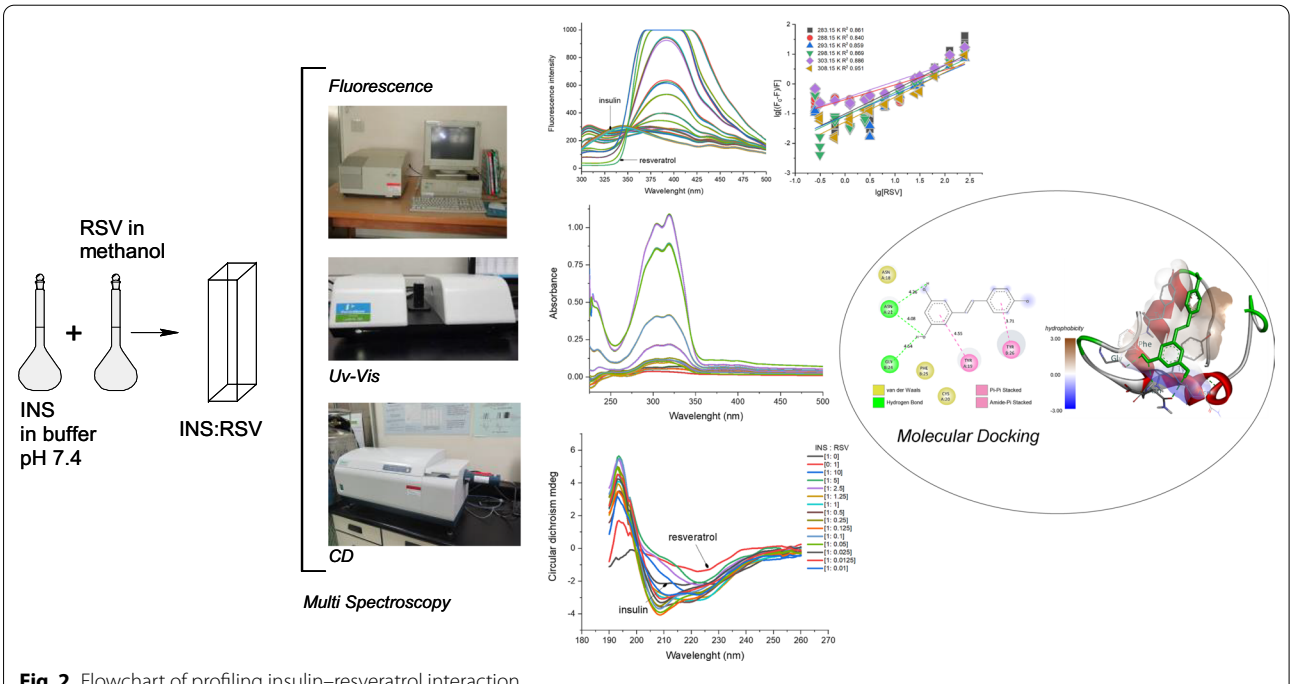

Fig. 2 Flowchart of profiling insulin–resveratrol interaction

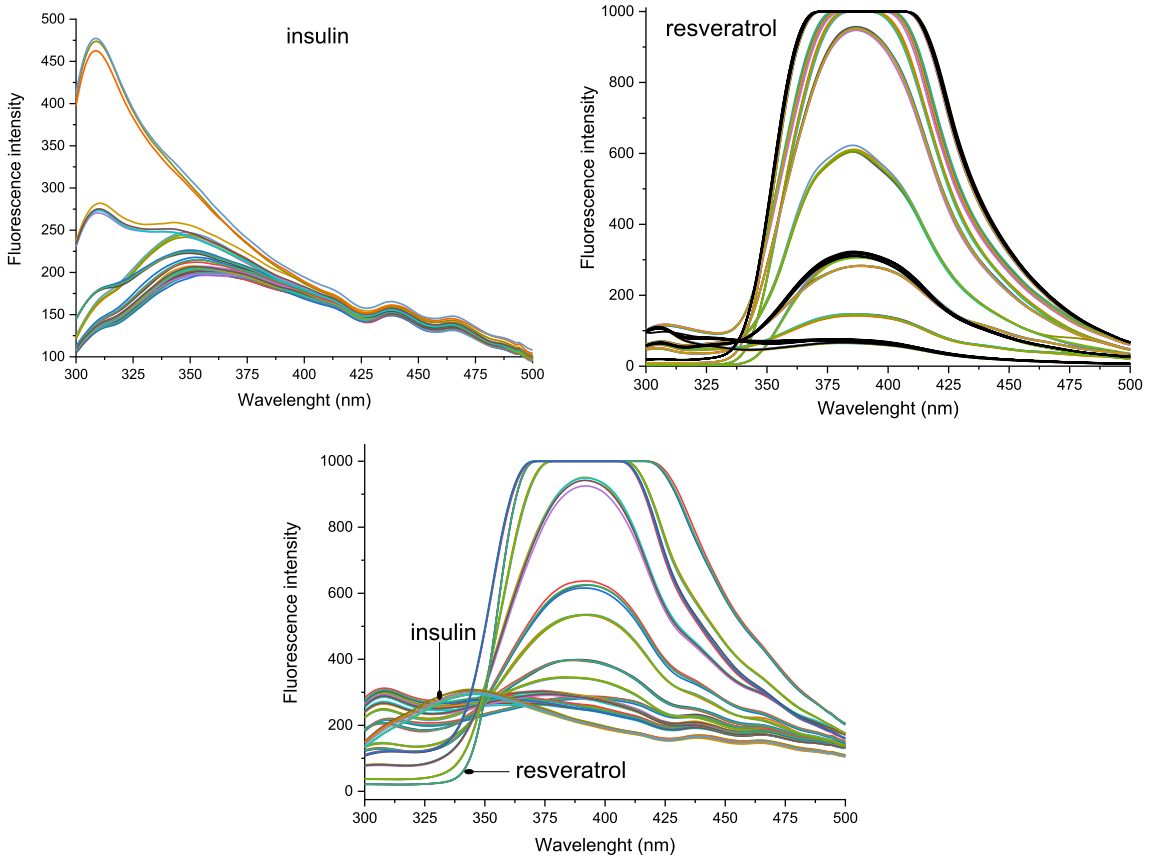

Fig. 3 Emission spectra of **a** insulin, **b** resveratrol, and **c** INS-RSV solution in different resveratrol ratios: excitation wavelength 280 nm, data pitch 1 nm, bandwidth at 5 nm, medium sensitivity mode, scanning 250 nm/min at 190–500 nm

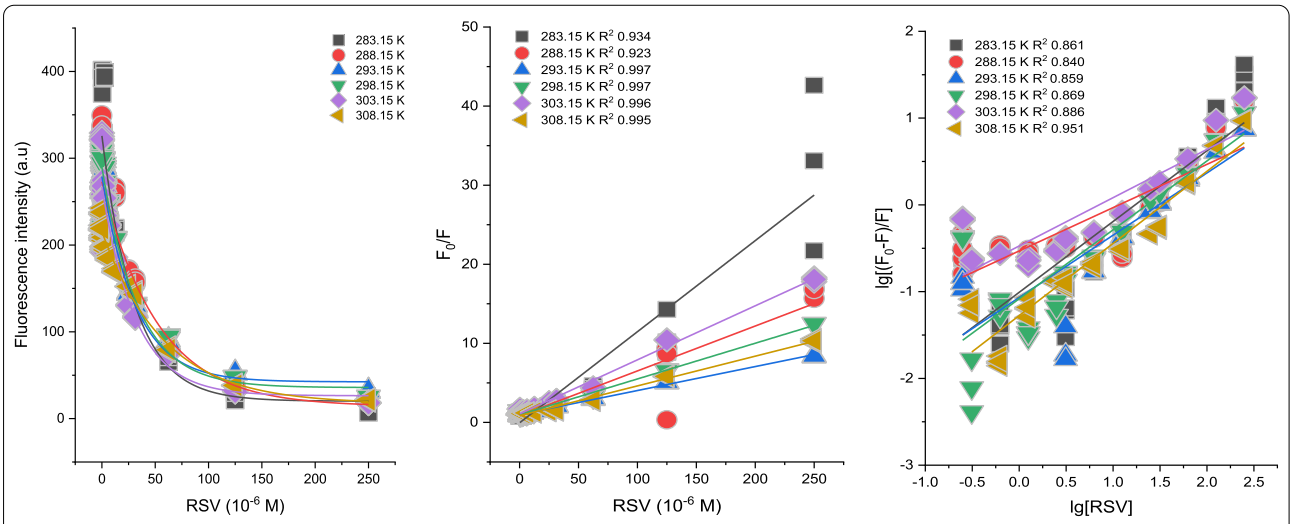

Fig. 4 **a** Fluorescence intensity of INS-RSV solution in different resveratrol ratios, **b** Stern–Volmer plot, and **c** double-logarithm plot of INS-RSV solution

Table 1 Thermodynamic and kinetic parameters of insulin and resveratrol interaction

Parameter	Unit	283.15 K	288.15 K	293.15 K	298.15 K	303.15 K	308.15 K
Dynamic quenching effect							
K_D	10^4 M^{-1}	11.5	5.68	3.03	4.52	6.83	3.76
k_{qD}	10^{13} M^{-1} s^{-1}	2.26	1.11	0.595	0.886	1.34	0.737
ΔG	kj mol^{-1}	12.955	12.836	12.717	12.597	12.478	12.359
ΔH	kj mol^{-1}	19.698					
ΔS	J $mol^{-1}K^{-1}$	23.814					
Static quenching effect							
K_s	10^5 M^{-1}	− 10.1	− 5.31	− 10.7	− 10.8	− 4.74	− 12.8
k_{qS}	10^{14} M^{-1} s^{-1}	− 1.98	− 1.04	− 2.09	− 2.12	− 0.929	− 2.50
n		0.816	0.499	0.718	0.794	0.557	0.831
ΔG	kj mol^{-1}	− 38.680	− 39.304	− 39.929	− 40.553	− 41.177	− 41.801
ΔH	kj mol^{-1}	− 3.341					
ΔS	J $mol^{-1}K^{-1}$	124.810					

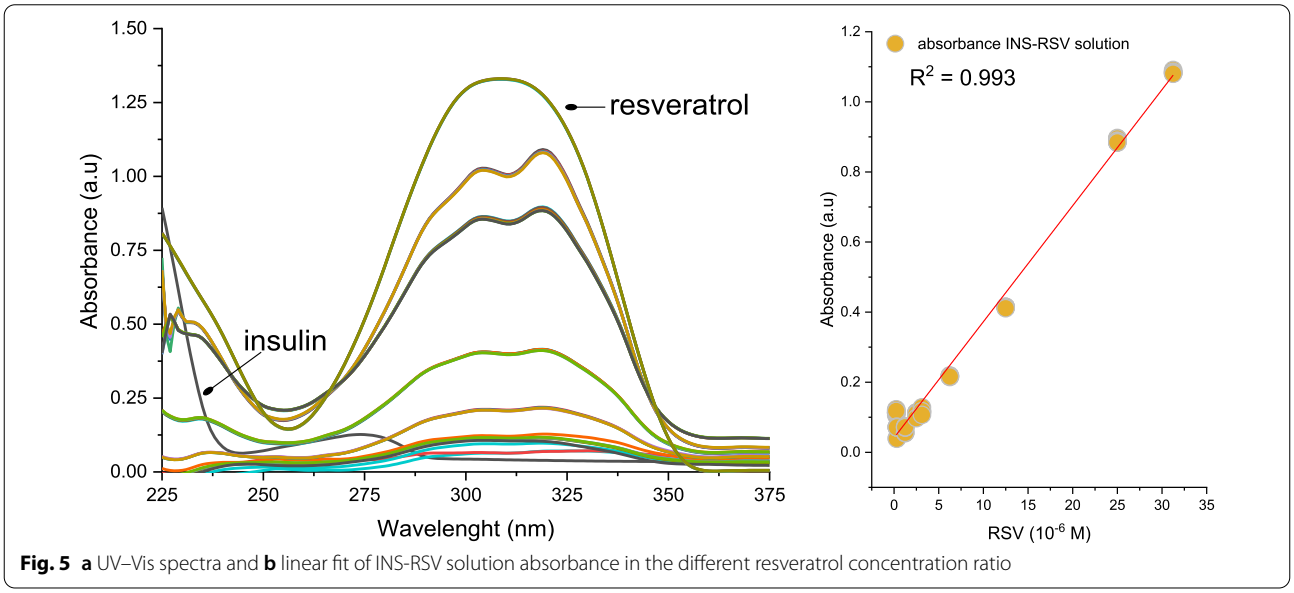

Fig. 5 **a** UV–Vis spectra and **b** linear fit of INS-RSV solution absorbance in the different resveratrol concentration ratio

fluorescence can emit light in the visible region (380–780 nm) [36]

Adding a quencher causes a decrease in fluorescence intensity, known as quenching [37]. In the interaction of insulin and resveratrol, resveratrol is a quencher. Quenchers are ligands, or guests, while insulin is called a fluorophore or host. The host is an organic molecule, having a hollow structure where the guest is bound. The bond that occurs between host and guest is weak and non-covalent. The process of forming the host–guest complex and the self-assembly are supramolecular concepts [38]. The emission spectra in Fig. 3 show that chain B insulin and resveratrol both have emission peaks. However, at the same concentration, the fluorescence intensity of resveratrol was higher than insulin. This indicates that resveratrol is more sensitive to visible light. The insulin emission disappears with the highest resveratrol concentration in the INS-RSV solution. Resveratrol has been reported having a sensitivity to UV light at 6 watts, temperature 295 K at a wavelength of 305 nm [39]. Fluorescence spectroscopy can identify electron transitions in aromatic functional groups.

Insulin has the aromatic amino acids tyrosine and phenylalanine, and tyrosine has a more remarkable fluorescence ability [33]. Aromatic functional groups have transitions π–π^* (phi or single bond) which are lower

Table 2 Molar absorptivity and maximum absorbance of INS-RSV solution

Solution	Concentration (10^{-5} M)	Absorbance	ε (M^{-1} cm^{-1})	λ max (nm)
Insulin	5.00	0.035	698.145	296
1: 0.01	0.00250	0.114	457,373.333	332
1: 0.0125	0.00313	0.054	173,411.556	326
1: 0.05	0.125	0.065	51,859.429	330
1: 0.1	0.250	0.109	43,745.600	320
1: 0.125	0.313	0.116	37,204.267	318
1: 0.25	0.625	0.217	34,677.440	319
1: 0.5	1.25	0.413	33,067.867	319
1:1	2.50	0.889	35,548.457	319
1: 1.25	3.13	1.084	34,693.333	319
Resveratrol	5.00	1.330	26,593.920	309

ε, Extinction coefficient, λ, Wavelength

in energy than σ–σ^* (sigma or double bonds). So the phi transition is more dominant than the sigma transition. In the emission state, there is a transition π^*–n or π^*–π. The choice is based on the lowest energy. Substitution of the benzene ring causes a shift in the maximum absorption wavelength, which impacts changes in fluorescence emission [40].

Observation of insulin using fluorescence shows that insulin at low concentrations had an emission peak of 362 nm; the other small peaks were 438 nm and 466 nm. At higher insulin concentrations, the emission peaks shifted to the lowest wavelengths, i.e., from 362 nm, 356 nm, 349 nm, 341 nm, 310 nm to 309 nm. This indicates that the buffer causes the insulin emission process to a blueshift. Insulin has been observed to have a maximum excitation peak at 280 nm [33]. This peak develops from the electron excitation of the aromatic amino acid functional group in the insulin structure. Insulin is composed of 4 amino acids as tyrosine residue and 3 as phenylalanine residue. Compared to phenylalanine, tyrosine has a dominant peak; therefore, tyrosine can be used as a reference for insulin fluorescence spectra [33]. The benzene (C_6H_6) functional group has fluorescence spectra at 270 -310 nm, while benzoic acid has a broad peak at 310–390 nm [40]. This study set up the excitation wavelength at 280 nm as per the previous studies. The maximum wavelength excitation for the insulin fluorescence study was 280 nm [33]. Insulin has an emission peak in the range of 309–362 nm.

Resveratrol consists of only two emission peaks, as shown in Fig. 3b. At low concentrations, it has emission peaks at 305 nm, 316 nm, and 377 nm. At a higher resveratrol concentration in the solution, the peak at 377 nm shifted to 387 nm, while peaks at 305 and 316 nm disappeared. Methanol causes the emission peak to become redshift. The phenol functional group (C_6H_5OH) is present in the resveratrol molecule. Phenol has a wavelength of 285–365 nm and a phenolate ion at 310–400 nm [40]. Peaks identical to resveratrol were found at 305, 315, and 404 nm [4].

The INS-RSV solution has an emission pattern similar to resveratrol, with two peaks at 306–308 nm and 392–394 nm (Fig. 3c). At a low resveratrol ratio, a new peak was found at 345–349 nm. The peak disappears as the resveratrol ratio increases. Other peaks detected in the INS-RSV solution were at 436 nm and 462 nm belonging to insulin emission. Another change at a higher molar

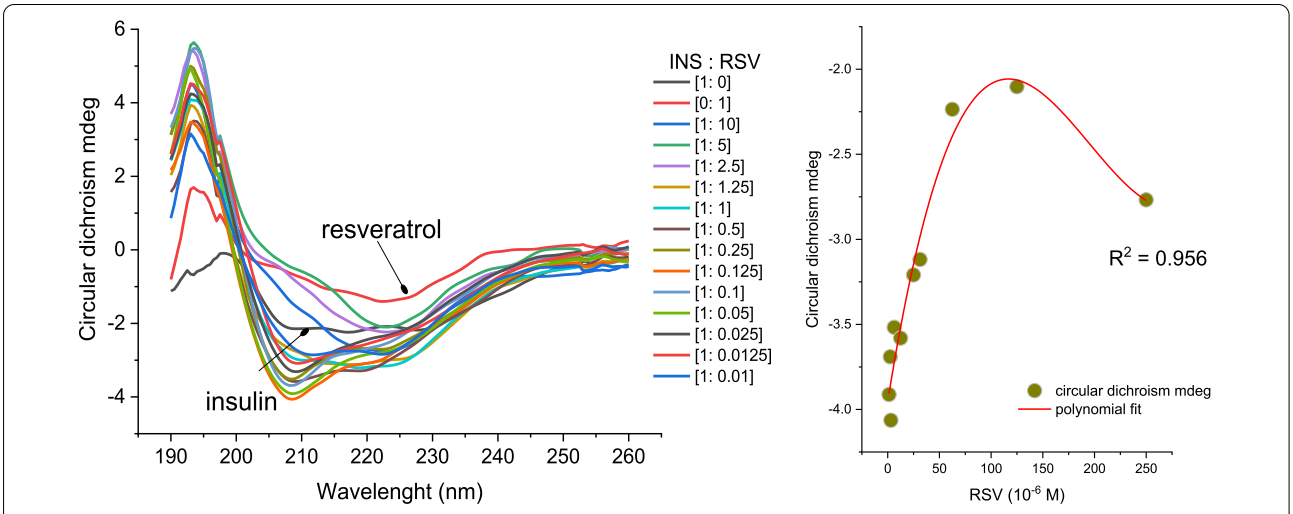

Fig. 6 **a** Circular dichroism spectra and **b** polynomial fit of circular dichroism millidegrees in INS-RSV solution, set in a bandwidth of 1 nm, standard sensitivity mode, data pitch of 0.5 nm, scanning 50 nm/min, continuous scan mode, range 190–260 nm

Table 3 The amount and length of secondary structure in INS-RSV solution

INS-RSV	α-Helix		β-Sheet and others	
	(Per 100 residues)	Length (Å)	(Per 100 residues)	Length (Å)
1:10	1.497	6.954	3.851	5.369
1:5	1.039	6.84	4.317	5.264
1:2.5	1.297	6.71	4.152	5.185
1:1.25	1.612	7.049	3.349	5.267
1:1	1.47	6.691	3.184	5.367
1:0.5	1.411	6.855	3.07	5.262
1:0.25	1.664	7.117	4.195	5.44
1:0.125	1.481	6.805	3.339	5.325
1:0.1	1.226	6.635	3.358	5.115
1:0.05	1.615	6.881	3.683	5.267
1:0.025	1.197	6.706	3.641	4.969
1:0.0125	1.261	6.604	3.694	5.191
1:0.01	1.582	7.018	3.825	5.441
1:0	2.379	4.465	5.48	4.819

ratio of resveratrol noted was that the 394 nm shifted to 392 nm, and 308 nm shifted to 306 nm. It indicates that the addition of the resveratrol ratio causes the main peak in insulin emission to decrease or disappear, or a red-shift peak shift in emission. The protein binding process with the ligand causes quenching and is characterized by peak shifts and decreased fluorescence intensity [27]. The decrease in fluorescence intensity can be seen in Fig. 4a. In the temperature range of 283.15 K, 288.15 K, 293.15 K, 298.15 K, 303.15 K, and 308.15 K, the fluorescence intensity of the INS-RSV solution decreased exponentially as the resveratrol concentration increased, with an $R^2 = 0.881–0.980$. This shows that the presence of resveratrol has succeeded in changing the microenvironment of insulin residues and quenching the insulin emission. This phenomenon is called quenching effect. Insulin has a drastic quenching effect when interacting with indole butyric acid (IBA). The tyrosine residue (A14, A19, B16, B12) is suspected in the involvement of changing this emission peak [29].

Three possible quenching effects occur in the interaction of the protein with ligands, namely static quenching, dynamic quenching, and a combination of both. Determination of quenching constant for dynamic quenching K_D can be performed using Stern–Volmer equation (Eq. 1 and Eq. 2). The linear regression of F_0/F and [RSV] produces a slope. The slope is quenching constant dynamic or K_D.

$$F_0/F = (F_0/F)_{obs} \times \eta = 1 + k_q \cdot \tau_0 \cdot [RSV] \quad (1)$$

$$K_D = k_{qD} \cdot \tau_0 \quad (2)$$

K_D values were observed at the different temperatures, as shown in Fig. 4b and Table 1. The dynamic quenching of insulin and resveratrol has a pattern that the higher the temperature, the K_D and the constant rate (k_{qD}) also decreased. The interaction was endothermic ($\Delta H > 0$) and not spontaneous ($\Delta G > 0$). Without the quencher, the tyrosine residue has a lifetime of 5.1 ns [4, 41]. In the quenching effect, the electron density in the aromatic ring of tyrosine was more influential than – CONH and – COOH. The electron density increased due to the addition of phenolic compounds [41].

The static quenching effect on the interaction of phloretin with insulin has the following characteristics: The two molecules are close together with weak interaction stability [33]. Table 1 shows the static quenching effect in the interaction of insulin and resveratrol, which is spontaneous, exothermic, and a decrease in the rate constant (k_{qS}), and decrease in the K_S at a higher temperature. The K_S is called the quenching constant of the static quenching effect and the binding constant. The K_S value is obtained from the intercept of the linear regression equation lg $[(F_0 - F)/F]$ with lg [RSV] (Fig. 4 and Eq. 3). The number of binding sites (n) is derived from the slope, its approximately one (Table 1)

$$\lg [(F_0 - F)/F] = \lg K_S + n \cdot \lg [RSV] \quad (3)$$

$$K_S = k_{qS} \cdot \tau_0 \quad (4)$$

$$\Delta G = \Delta H - T \cdot \Delta S. \quad (5)$$

Thermodynamic parameters such as enthalpy ΔH and entropy (ΔS) are obtained from the van't Hoff equation [42]. $\ln K$ and $1000/T$ linear regression produce the slope value as $\Delta H/R$ and intercept as $\Delta S/R$. Determination of Gibbs energy (ΔG) using Eq. 5. Compared with the maximum dynamic quenching rate 2.0×10^{10} M^{-1} s^{-1} [4, 43, 44], the quenching constant rate of INS-RSV interaction is greater than the maximum dynamic quenching rate. A higher quenching rate indicates that the quenching of the two molecules takes place rapidly, but it decreases with increasing temperature (Table 1). Therefore, the quenching effect in INS-RSV interaction was a combined quenching effect. The interaction begins spontaneously, at a fast rate in the static quenching stage, followed by a non-spontaneous reaction in dynamic quenching at a slower rate as the temperature increases.

Based on the enthalpy (ΔH) and entropy (ΔS) values, interaction is classified into several types: hydrophobic if $\Delta H > 0$, $\Delta S > 0$. If $\Delta H < 0$, $\Delta S < 0$ were hydrogen bonds and dispersion forces. If $\Delta H \cong 0$, $\Delta S < 0$, then it

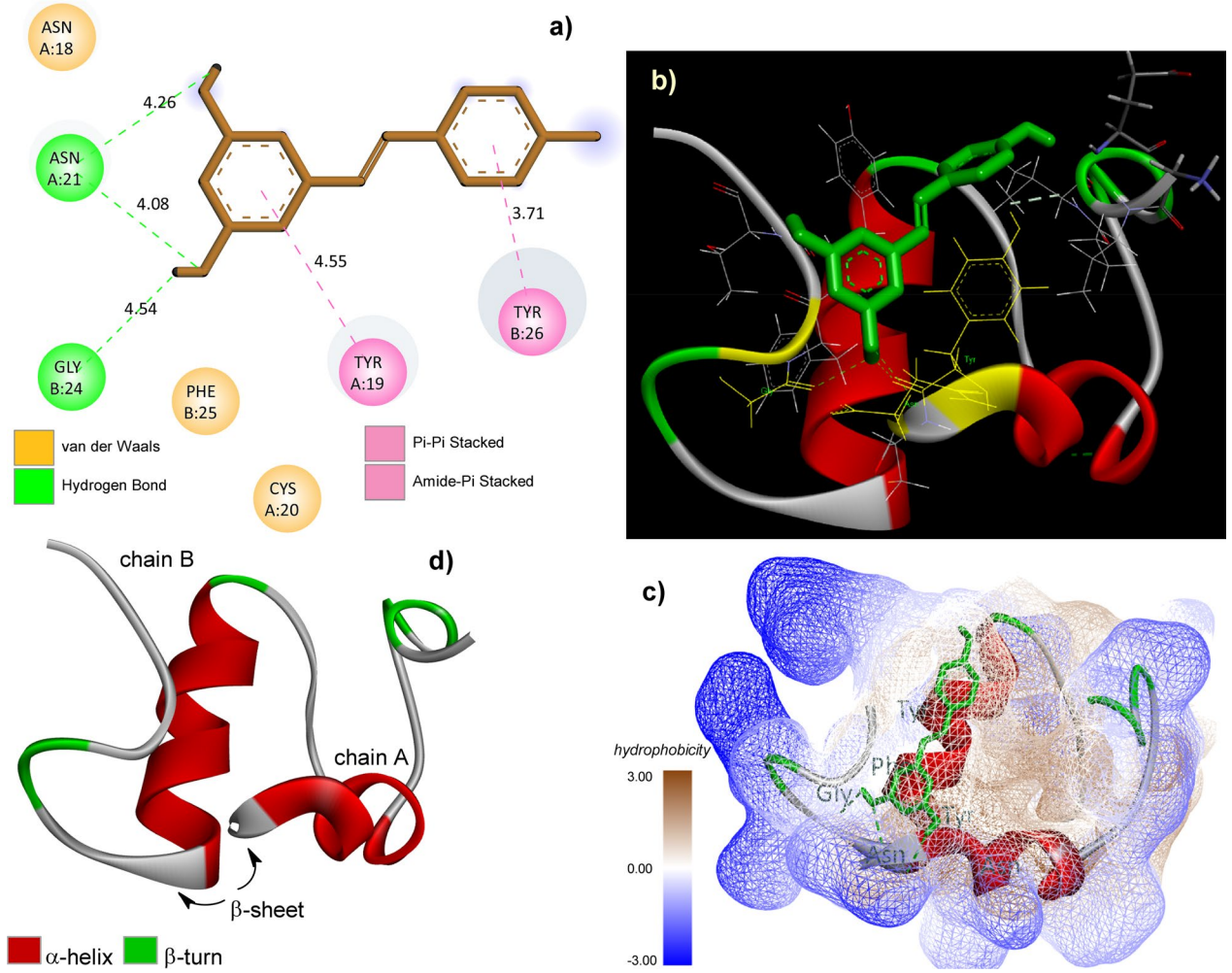

Fig. 7 Visualization of **a** binding residue INS-RSV, **b** binding residue with insulin secondary structure, **c** binding site INS-RSV with hydrophobicity surface region, and **d** secondary structure of insulin

Table 4 The binding energy of insulin and resveratrol using AutoDock Vina

Mode	Affinity (kcal/mol)	Distance from best mode (Å)	
		rmsd l.b	rmsd u.b
1	−6.3	0	0
2	−6.2	0.037	2.014
3	−5.9	2.113	2.891
4	−5.8	1.255	7.527
5	−5.6	1.671	7.497
6	−5.6	1.705	7.271
7	−5.5	3.843	6.878
8	−5.5	3.291	3.939
9	−5.4	1.939	2.799

rmsd, Root-mean-square deviation; l.b, Lower bound; and u.b, Upper bound

is electrostatic interaction. If $\Delta H\langle 0, \Delta S\rangle 0$, it is categorized as an electrostatic interaction [42]. The energy transfer from a cold to a hot temperature can change the entropy value. The standard entropy of a gas is positive. A negative value appears if the gas is converted to a liquid [45]. The standard entropy of water in the solid state is 45 J mol^{-1} K^{-1}. In the liquid state, water has an entropy value of 70 J mol^{-1} K^{-1}[46]. Based on the data in Table 1, the entropy value of the INS-RSV is 23.814–124.810 J mol^{-1} K^{-1}. This indicates the condition of INS-RSV has a liquid phase, but the molecular density is less than water molecules in general. The interaction of insulin is hydrophobic, electrostatic, and has hydrogen bonds, and also, there are dispersion forces between insulin and resveratrol molecules.

4.2 UV–Vis spectroscopy

At lower concentrations, insulin has absorbance peaks at 257 nm and 291 nm. At a higher insulin concentration, the absorbance peak shifts from 291 to 274 nm, and the high-intensity peak appears at 220 nm. Insulin has maximum peaks at 276 nm, and 283 nm belongs to tyrosine and phenylalanine [4]. The 220 nm peak signals the protein chromophore group [47]. The absorption of insulin in various solvents was detected at 250–300 nm. In contrast to protamine, insulin has a positive charge at pH 7 [48]. The endocrine pancreas has the physiological condition for native insulin at pH 7.4 [49]. The peak of insulin absorption in the INS-RSV solution was the smallest. Resveratrol at the lowest concentration 5.0×10^{-7} M had small peaks at 256 nm, 294 nm, and 329 nm. The peak at 5.0×10^{-6} M concentration was detected at 301 nm. The concentrations of 5.0×10^{-5} M to 1.25×10^{-4} M peaked at 308 nm (Fig. 5).

It has been reported earlier that when interacting with insulin, resveratrol's proprietary peaks appeared at 305 nm and 315 nm [4]. In our study, the 1:001 resveratrol ratio peaked at 254 nm, 304 nm, and 332 nm, while the 1:1 ratio peaks at 305 nm and 320 nm. The ratio 1:0.5, 1:1, 1:1.25 peaks at 305 nm and 319 nm. The results on the effects of resveratrol on insulin are given in Table 2 and Fig. 5. A higher resveratrol ratio has led to the following conditions: the disappearance of the insulin peak, higher absorbance of INS-RSV, and a low extinction coefficient, and the maximum peak of INS-RSV shifts to a lower wavelength. The shift of the peak to a lower wavelength position is called the blueshift. The blueshift is also referred to as hypochromic [40]. Verdian and Housaindokht reported that a higher insulin concentration in INS-IBS causes hypochromic events [29]. At a higher resveratrol concentration, the absorbance of the INS-RVS solution is hypochromic (shift from 332 to 319 nm). Absorbance intensity and concentration ratio of resveratrol have a positive correlation, and mean increase in resveratrol has effect high of absorbance intensity (Fig. 5b).

Insulin is composed of a chromophore group (C = C) packed in an aromatic amino acids structure. The chromophore functional group is a covalent unsaturated group (π orbital) responsible for the absorption of insulin molecules. Chromophore groups are usually found in complex molecules [40]. Resveratrol has an auxochrome (− OH) group packed into a phenolic structure. Conjugation of an auxochrome group with a chromophore can change the absorbance intensity and the position of the maximum wavelength. The extinction coefficient of insulin is lower than resveratrol, indicating that the number of transition electrons ($\pi \rightarrow \pi^*$) in the insulin molecule is less than resveratrol. This causes the pattern of INS-RSV solution spectra to be similar to resveratrol spectra. The addition of resveratrol causes the number of electron transitions in the insulin molecule to decrease, suggesting that the insulin molecule interacts with resveratrol. The electron transition in aromatic hydrocarbons occurs in the $\pi \rightarrow \pi^*$ orbitals [40].

4.3 Circular dichroism spectropolarimeter

The characteristic CD spectra depend on secondary structure confirmation. One of the factors that cause conformational changes is binding interaction with ligands [35, 50]. The secondary structure of insulin can change with the appearance of ligands such as surfactants [35].

Figure 6a shows that insulin has a negative signal at 209 nm, 217 nm, and 227 nm. In earlier reports, the α-helix had a positive peak at 193 nm, negative at 208 nm, and 222 nm [27, 33]. Small peaks belonging to β-sheet and others have a positive peak at 195 nm and negative at 218 nm [24, 50, 51]. A negative peak at 209 nm is still visible at a lower resveratrol concentration ratio. The addition of the resveratrol ratio causes the peak shift to 211 nm. The peak at 217 nm shifts to 219 nm. The higher resveratrol ratio causes the INS-RSV peak at 222 nm to be broad range spectra. Resveratrol has a wide negative peak at 222 nm. Figure 6b shows at a lower concentration of resveratrol have a linear correlation with ellipticity, which is reported as millidegrees (mdeg). Meanwhile, higher resveratrol concentrations have a polynomial correlation with ellipticity. The highest resveratrol concentration reduces the ellipticity of the INS-RSV solution. This means interaction of the secondary structure of insulin can be optimum at a lower concentration ratio of resveratrol.

The interaction of insulin with resveratrol has changed the conformation of insulin through changes in the secondary structure stability. Ligands in tocopherol compounds can stabilize the insulin structure [27]. Paclitaxel can change the insulin monomer structure to become fibrillated. This was observed by shifting the CD spectra [24]. The online determination method has been used to determine the second amount of insulin per 100 residues and the length of the structure (Table 2). Based on these data, the addition of resveratrol has changed the secondary structure of insulin, which is slightly increased the amount of α-helix and slightly reduces β-sheet and other structures. There was an increase in the length of the secondary structure. This means that the secondary structure in insulin becomes longer by adding resveratrol. Changes in peptide length play an important role in the stability of molecular and geometric structures. The

helix-to-sheet transition depends on how fast the helix is affected by the bioinspired material [52].

4.4 Molecular docking

Profiling of the binding site position and binding residue in 3D, a molecular docking study was conducted. The insulin interaction with resveratrol involves hydrogen bonding of glycine (GLY24) chain B and asparagine (ASN21) chain B. The electron density in the aromatic ring tyrosine (TRY19) chain A and tyrosine (TRY26) chain B is affected by resveratrol's benzene ring. The electrons interact through the $\pi \rightarrow \pi$ orbitals between TRY and resveratrol. The ASN18 residues, phenylalanine (PHE25), and cysteine (CYS20) interact with resveratrol via van der Waals interaction (Fig. 7a).

The position of the binding site is between the two helix chains A and B (Fig. 7bc), causing the helix structure to change. The CD spectra increase the length of the insulin secondary structure (Fig. 6, Table 2). The binding site has a region in the range of hydrophobicity -3.00 to 3.00. Hydrophobicity and energy binding have important roles in drug efficacy. The interaction flexibility is influenced by water molecules [53]. Hydrophobicity can affect the value of ΔS [46]. INS-RSV solution has a value of $\Delta S > 0$, indicating that the molecules are at liquid–gas phase condition. Figure 7a, c shows the solvent effect in the high hydrophobicity surface area, specifically at the phenolic and tyrosine interaction regions. It is marked with a gray to bluish-gray color. Hydrogen bonding occurs in the low hydrophobicity region because the presence of water molecules can inhibit the formation of resveratrol bonds with insulin.

The affinity energy involved in the INS-RSV interaction is about -6.3 to -5.4 kcal/mol. Affinity is also called the binding energy between insulin and resveratrol. A negative affinity value indicates that the interaction occurs spontaneously, supported by the ΔG value in Table 1. The binding energy increases with the longer distance between resveratrol and insulin. The best resveratrol conformation for binding is the first mode conformation, because the closest the distance , the lowest the energy affinity. The lowest of root-mean-square deviation (rmsd) means great stability [54]. Resveratrol has nine possible conformational forms when interacting with insulin (Table 4).

5 Conclusions

Profiling of insulin and resveratrol interactions was carried out using multi-spectroscopy and molecular docking methods. Spectroscopy methods used were fluorescence spectroscopy, ultraviolet–visible (UV–Vis) spectroscopy, and circular dichroism (CD) spectropolarimeter. Investigation of binding sites and binding residues was done by molecular docking. The addition of resveratrol affects insulin emission. The fluorescence spectroscopy results showed that the peak of insulin emission was reduced. Resveratrol causes insulin emission to become quenching. The increase in temperature causes the binding constant and the binding site to be unstable. The interaction of insulin and resveratrol involves hydrogen bonds, van der Waal, and is hydrophobic. The results of UV–Vis spectroscopy showed a high resveratrol ratio caused the peak to become a blueshift, the absorbance to become hyperchromic, and a decrease in the extinction coefficient. The results of the CD spectropolarimeter showed that resveratrol affected the amount and the length of the secondary structure of insulin. Molecular docking investigated resveratrol interaction via hydrogen bonds, van der Waal bonds, and phi orbital interactions. The binding residues consist of glycine, asparagine, phenylalanine, cysteine, and tyrosine as insulin residues. The interaction of the two molecules occurs spontaneously in the hydrophobic area. Profiling of the interaction of insulin and resveratrol shows that resveratrol can stabilize insulin structure and prevent insulin resistance in diabetes.

Abbreviations

INS: Insulin; RSV: Resveratrol; UV–Vis: Ultraviolet–visible; CD: Circular dichroism; T2D: Type 2 diabetes; GLY: Glycine; ASN: Asparagine; TRY: Tyrosine; PHE: Phenylalanine; CYS: Cysteine.

Acknowledgements

The authors would like to thank you for the support of the Department of Applied Chemistry Chaoyang University of Technology, Taiwan.

Author contributions

SY conceived the idea, developed the theory, carried out the experimental work, collected the data, analyzed the data, and drafted the manuscript. WJC contributed to funding acquisition sources and supervised the research work. DCA revised the draft and made a substantial contribution to the manuscript. All authors agree to submit the manuscript. All authors read and approved the final manuscript.

Funding

This research was funded by the Department of Applied Chemistry Chaoyang University of Technology, Taiwan.

Availability of data and materials

The authors confirm that the data supporting this study's findings are available within the article and its supplementary materials.

Declarations

Ethics approval and consent to participate

Not applicable.

Consent for publication

Not applicable.

Competing interests

The authors declare that they have no competing interests.

Author details
[1]Department of Applied Chemistry, Chaoyang University of Technology, 168, Jifeng E. Rd., Wufeng District, Taichung City 413310, Taiwan. [2]Department of Agricultural Product Technology, Sumbawa University of Technology, Sumbawa Besar, Olat Maras Rd. Moyo Hulu, West Nusa Tenggara, 84371, Indonesia. [3]Department of Environmental Engineering and Management, Chaoyang University of Technology, 168, Jifeng E. Rd., Wufeng District, Taichung City 413310, Taiwan.

Received: 22 February 2022 Accepted: 4 July 2022
Published online: 23 July 2022

References

1. Delpino FM, Figueiredo LM (2021) Resveratrol supplementation and type 2 diabetes: a systematic review and meta-analysis. Crit Rev Food Sci Nutr. https://doi.org/10.1080/10408398.2021.1875980
2. Gambini J, Inglés M, Olaso G, Lopez-Grueso R, Bonet-Costa V, Gimeno-Mallench L, Borras C (2015) Properties of resveratrol: in vitro and in vivo studies about metabolism, bioavailability, and biological effects in animal models and humans. Oxid Med Cell Longev. https://doi.org/10.1155/2015/837042
3. Harney TL (2021) Evaluation of trans-resveratrol as a treatment for periodontitis. In: Oral health care, pp 1–23. IntechOpen. https://doi.org/10.5772/intechopen.101477
4. Chen YY, Xiao L, Cui JH, Chen GF, Zhang J, Wang P (2013) Biological relevance of the interaction between resveratrol and insulin. Food Biophys 8(4):282–289. https://doi.org/10.1007/s11483-013-9301-8
5. She QB, Ma WY, Wang M, Kaji A, Ho CT, Dong Z (2003) Inhibition of cell transformation by resveratrol and its derivatives: differential effects and mechanisms involved. Oncogene 22(14):2143–2150. https://doi.org/10.1038/sj.onc.1206370
6. Takaoka M (1939) The phenolic substances of white Hellebore (*Veratrum grandiflorum* Loes fil.) II. Nippon Kagaku Kaishi 60(12):1261–1264. https://doi.org/10.1246/nikkashi1921.60.1261
7. Alesci A, Nicosia N, Fumia A, Giorgianni F, Santini A, Cicero N (2022) Resveratrol and immune cells: a link to improve human health. Molecules 27(2):1–19. https://doi.org/10.3390/molecules27020424
8. Han WC, Shi N, Wang XY, Wang ZH, Wang KL, Gao M, Xu X (2021) Application of natural cotton fibers as an extraction sorbent for the detection of trans-resveratrol in adulterated peanut oils. Food Chem 339(February 2020):127885. https://doi.org/10.1016/j.foodchem.2020.127885
9. Sanders TH, McMichael RW, Hendrix KW (2000) Occurrence of resveratrol in edible peanuts. J Agric Food Chem 48(4):1243–1246. https://doi.org/10.1021/jf990737b
10. Aljuhaimi F, Özcan MM (2018) Influence of oven and microwave roasting on bioproperties, phenolic compounds, fatty acid composition, and mineral contents of nongerminated peanut and germinated peanut kernel and oils. J Food Process Preserv. https://doi.org/10.1111/jfpp.13462
11. Uslu N, Özcan MM (2019) Effect of microwave heating on phenolic compounds and fatty acid composition of cashew (*Anacardium occidentale*) nut and oil. J Saudi Soc Agric Sci 18(3):344–347. https://doi.org/10.1016/j.jssas.2017.10.001
12. Gómez-Zorita S, Fernández-Quintela A, Lasa A, Hijona E, Bujanda L, Portillo MP (2013) Effects of resveratrol on obesity-related inflammation markers in adipose tissue of genetically obese rats. Nutrition 29(11–12):1374–1380. https://doi.org/10.1016/j.nut.2013.04.014
13. Mir SA, Shah MA, Ganai SA, Ahmad T, Gani M (2019) Understanding the role of active components from plant sources in obesity management. J Saudi Soc Agric Sci 18(2):168–176. https://doi.org/10.1016/j.jssas.2017.04.003
14. Zhu X, Wu C, Qiu S, Yuan X, Li L (2017) Effects of resveratrol on glucose control and insulin sensitivity in subjects with type 2 diabetes: systematic review and meta-analysis. Nutr Metab 14(1):1–10. https://doi.org/10.1186/s12986-017-0217-z
15. Nolan CJ, Prentki M (2019) Insulin resistance and insulin hypersecretion in the metabolic syndrome and type 2 diabetes: time for a conceptual framework shift. Diab Vasc Dis Res 16(2):118–127. https://doi.org/10.1177/1479164119827611
16. Kong L, Chen X, Gissler M, Lavebratt C (2020) Relationship of prenatal maternal obesity and diabetes to offspring neurodevelopmental and psychiatric disorders: a narrative review. Int J Obes 44(10):1981–2000. https://doi.org/10.1038/s41366-020-0609-4
17. American Diabetes Association; Centers for Disease Control and Prevention (2022) National diabetes statistics report: estimates of diabetes and its burden in the epidemiologic estimation methods. National Diabetes Statistics Report. http://www.cdc.gov/diabetes/pubs/statsreport14/national-diabetes-report-web.pdf
18. Kumar S, Kumar P, Nair MS (2021) Exploring the binding of resveratrol to a promoter DNA sequence d(CCAATTGG)2 through multispectroscopic, nuclear magnetic resonance and molecular dynamics studies. Spectrochim Acta Part A Mol Biomol Spectrosc 252:1–49. https://doi.org/10.1016/j.saa.2021.119488
19. Ren G, Sun H, Guo J, Fan J, Li G, Xu S (2019) Molecular mechanism of the interaction between resveratrol and trypsin: via spectroscopy and molecular docking. Food Funct 10(6):3291–3302. https://doi.org/10.1039/c9fo00183b
20. Jiang XY, Li WX, Cao H (2008) Study of the interaction between trans-resveratrol and BSA by the multi-spectroscopic method. J Solut Chem 37(11):1609–1623. https://doi.org/10.1007/s10953-008-9323-x
21. Nair MS (2015) Spectroscopic study on the interaction of resveratrol and pterostilbene with human serum albumin. J Photochem Photobiol, B 149:58–67. https://doi.org/10.1016/j.jphotobiol.2015.05.001
22. Szkudelska K, Deniziak M, Sassek M, Szkudelski I, Noskowiak W, Szkudelski T (2021) Resveratrol affects insulin signaling in type 2 diabetic goto-kakizaki rats. Int J Mol Sci 22(5):1–15. https://doi.org/10.3390/ijms22052469
23. Maier R, Fries MR, Buchholz C, Zhang F, Schreiber F (2021) Human versus bovine serum albumin: a subtle difference in hydrophobicity leads to large differences in bulk and interface behavior. Cryst Growth Des 21(9):5451–5459. https://doi.org/10.1021/acs.cgd.1c00730
24. Kachooei E, Moosavi-Movahedi AA, Khodagholi F, Mozaffarian F, Sadeghi P, Hadi-Alijanvand H, Sheibani N (2014) Inhibition study on insulin fibrillation and cytotoxicity by paclitaxel. J Biochem 155(6):361–373. https://doi.org/10.1093/jb/mvu012
25. Grasso EJ, Oliveira RG, Maggio B (2016) Surface interactions, thermodynamics and topography of binary monolayers of insulin with dipalmitoylphosphatidylcholine and 1-palmitoyl-2-oleoylphosphatidylcholine at the air/water interface. J Colloid Interface Sci 464:264–276. https://doi.org/10.1016/j.jcis.2015.11.034
26. Iannuzzi C, Borriello M, Irace G, Cammarota M, Maro AD, Sirangelo I, Sirangelo I (2017) Vanillin affects amyloid aggregation and non-enzymatic glycation in human insulin. Sci Rep. https://doi.org/10.1038/s41598-017-15503-5
27. Soleymani H, Saboury AA, Moosavi-Movahedi AA, Rahmani F, Maleki J, Yousefinejad S, Maghami P (2016) Vitamin E induces regular structure and stability of human insulin, more intense than vitamin D3. Int J Biol Macromol 93:868–878. https://doi.org/10.1016/j.ijbiomac.2016.09.047
28. Babenko V, Dzwolak W (2013) Amino acid sequence determinants in self-assembly of insulin chiral amyloid superstructures: role of C-terminus of B-chain in association of fibrils. FEBS Lett 587(6):625–630. https://doi.org/10.1016/j.febslet.2013.02.010
29. Verdian-Doghaei A, Housaindokht MR (2015) Spectroscopic study of the interaction of insulin and its aptamer—sensitive optical detection of insulin. J Lumin 159:1–8. https://doi.org/10.1016/j.jlumin.2014.10.025
30. Brange J, Langkjoer L (1993) Insulin structure and stability. Pharm Biotechnol 5:315–350. https://doi.org/10.1007/978-1-4899-1236-7_11
31. Gong Q, Zhang H, Zhang H, Chen C (2019) Calculating the absolute binding free energy of the insulin dimer in an explicit solvent. RSC Adv 10(2):790–800. https://doi.org/10.1039/c9ra08284k
32. Busto-Moner L, Feng CJ, Antoszewski A, Tokmakoff A, Dinner AR (2021) Structural ensemble of the insulin monomer. Biochemistry 60(42):3125–3136. https://doi.org/10.1021/acs.biochem.1c00583
33. Yanti S, Wu Z-W, Agrawal DC, Chien W-J (2021) Interaction between phloretin and insulin: a spectroscopic study. J Anal Sci Technol 12(1):34. https://doi.org/10.1186/s40543-021-00284-4
34. Day RA, Underwood AL (1998) Quantitative analysis, 6th edn. Prentice Hall, Englewood Cliffs

35. Pirhaghghi M, Saboury AA, Najafi F, Pourhosseini PS, Ghourchian H (2015) Biophysical studies on the interaction of insulin with a cationic gemini surfactant. J Sci Islam Repub Iran 26(2):105–115
36. Skoog DA, West DM, Holler FJ, Crouch SR (2014) Fundamentals of analytical chemistry. Cengage Learning Asia Pte Ltd, Taipei
37. Lakowicz JR (2006) Principles of fluorescence spectroscopy. In: Lakowicz JR (ed) Geofisica pura e applicata, vol 33, 3rd edn. University of Maryland School of Medicine Baltimore, Springer, Maryland
38. Ioele G, De Luca M, Garofalo A, Ragno G (2017) Photosensitive drugs: a review on their photoprotection by liposomes and cyclodextrins. Drug Delivery 24:33–44. https://doi.org/10.1080/10717544.2017.1386733
39. Yang I, Kim E, Kang J, Han H, Sul S, Park SB, Kim SK (2012) Photochemical generation of a new, highly fluorescent compound from non-fluorescent resveratrol. Chem Commun 48(32):3839–3841. https://doi.org/10.1039/C2CC30940H
40. Skoog DA, Holler FJ, Crouch SR (2007) Principles of instrumental analysis, 6th edn. Brooks/Cole Publishing, Cengage Learning, Berlin
41. Feitelson J (1969) Environmental effects on the fluorescence of tyrosine and its homologues. Photochem Photobiol 9(5):401–410. https://doi.org/10.1111/j.1751-1097.1969.tb07306.x
42. Alanazi MM, Almehizia AA, Bakheit AH, Alsaif NA, Alkahtani HM, Wani TA (2019) Mechanistic interaction study of 5,6-Dichloro-2-[2-(pyridin-2-yl) ethyl]isoindoline-1,3-dione with bovine serum albumin by spectroscopic and molecular docking approaches. Saudi Pharm J 27(3):341–347. https://doi.org/10.1016/j.jsps.2018.12.001
43. Blatt E, Chatelier RC, Sawyer WH (1986) Effects of quenching mechanism and type of quencher association on Stern–Volmer plots in compartmentalized systems. Biophys J 50(2):349–356. https://doi.org/10.1016/S0006-3495(86)83468-3
44. Gentili PL, Ortica F, Favaro G (2008) Static and dynamic interaction of a naturally occurring photochromic molecule with bovine serum albumin studied by UV–visible absorption and fluorescence spectroscopy. J Phys Chem B 112(51):16793–16801. https://doi.org/10.1021/jp805922g
45. Atkins P, Paula J (2010) Physical chemistry, 9th edn. Oxford University Press, New York
46. Li J, Hou C, Ma X, Guo S, Zhang H, Shi L, He X (2021) Entropy-enthalpy compensations fold proteins in precise ways. Int J Mol Sci 22(17):1–20. https://doi.org/10.3390/ijms22179653
47. Nienhaus K, Nienhaus GU (2005) Probing heme protein-ligand interactions by UV/visible absorption spectroscopy. Methods Mol Biol (Clifton NJ) 305:215–242. https://doi.org/10.1385/1-59259-912-5:215
48. Liefeng Z, Hui J, Wenjie Z, Lin W, Lingling S, Qiuyan W, Yong R (2008) Improving the stability of insulin in solutions containing intestinal proteases in vitro. Int J Mol Sci 9(12):2376–2387. https://doi.org/10.3390/ijms9122376
49. Sitkowski J, Bocian W, Bednarek E, Urbańczyk M, Koźmiński W, Borowicz P, Kozerski L (2018) Insight into human insulin aggregation revisited using NMR derived translational diffusion parameters. J Biomol NMR 71(2):101–114. https://doi.org/10.1007/s10858-018-0197-y
50. Greenfield NJ (2007) Using circular dichroism spectra to estimate protein secondary structure. Nat Protoc 1(6):2876–2890. https://doi.org/10.1038/nprot.2006.202
51. Iannuzzi C, Borriello M, Portaccio M, Irace G, Sirangelo I (2017) Insights into insulin fibril assembly at physiological and acidic ph and related amyloid intrinsic fluorescence. Int J Mol Sci. https://doi.org/10.3390/ijms18122551
52. Marullo R, Kastantin M, Drews LB, Tirrell M (2013) Peptide contour length determines equilibrium secondary structure in protein-analogous micelles. Biopolymers 99(9):573–581. https://doi.org/10.1002/bip.22217.Peptide
53. Patil R, Das S, Stanley A, Yadav L, Sudhakar A, Varma AK (2010) Optimized hydrophobic interactions and hydrogen bonding at the target-ligand interface leads the pathways of drug-designing. PLoS ONE. https://doi.org/10.1371/journal.pone.0012029
54. Nath A, Kumer A, Zaben F, Khan MW (2021) Investigating the binding affinity, molecular dynamics, and ADMET properties of 2,3-dihydrobenzofuran derivatives as an inhibitor of fungi, bacteria, and virus protein. Beni-Suef Univ J Basic Appl Sci. https://doi.org/10.1186/s43088-021-00117-8

Publisher's Note